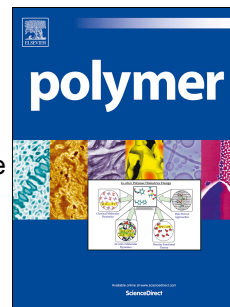# Accepted Manuscript

Glass-like transparent high strength polyethylene films by tuning drawing temperature

Yunyin Lin, Ruhi Patel, Jun Cao, Wei Tu, Han Zhang, Emiliano Bilotti, Cees W.M. Bastiaansen, Ton Peijs

Please cite this article as: Lin Y, Patel R, Cao J, Tu W, Zhang H, Bilotti E, Bastiaansen CWM, Peijs T, Glass-like transparent high strength polyethylene films by tuning drawing temperature, *Polymer* (2019), doi: https://doi.org/10.1016/j.polymer.2019.03.036.

Glass-like transparent high strength polyethylene films by tuning drawing temperature

Yunyin Lin [a], Ruhi Patel [a], Jun Cao [a], Wei Tu [b], Han Zhang [a,b], Emiliano Bilotti [a,b], Cees W. M. Bastiaansen *,[a,c], and Ton Peijs *,[d]

[a] School of Engineering and Materials Science, Queen Mary University of London, Mile End Road, London E1 4NS, U.K.

[b] Nanoforce Technology Ltd., Mile End Road, London E1 4NS, U.K.

[c] Laboratory of Functional Organic Materials and Devices, Eindhoven University of Technology, P.O. Box 513, Eindhoven 5600 MB, The Netherlands

[d] Materials Engineering Centre, WMG, University of Warwick, Coventry CV4 7AL, U.K.
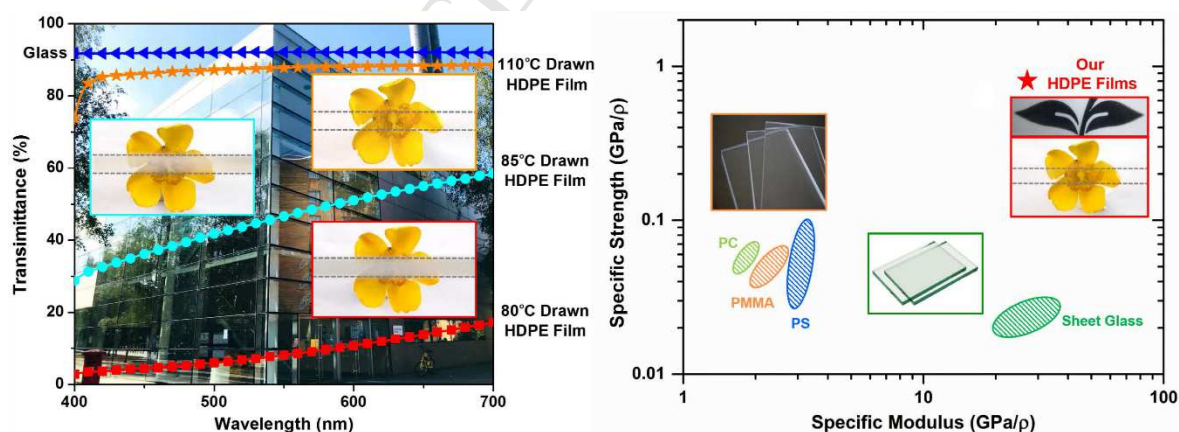
* Corresponding Authors.

E-mail address: t.peijs@warwick.ac.uk (T. Peijs) and c.w.m.bastiaansen@tue.nl (C.W.M. Bastiaansen).

Abstract

High performance transparent polymeric materials are of great interests in many fields including automotive and electronics. Conventional transparent plastics like polycarbonate (PC) and poly(methyl methacrylate) (PMMA) possess relatively unsatisfactory mechanical performance, while high performance polymeric systems like solid-state drawn high-density polyethylene (HDPE) typically have an opaque appearance, limiting applications where both mechanical and optical properties are required. In this study, we successfully combined high transparency and high strength in HDPE films by carefully controlling processing parameters

1

during solid-state drawing. By tuning the drawing temperature, highly oriented HDPE films with a transmittance of ~ 90 % are achieved even in the far field. Greater chain mobility at high drawing temperatures is believed to be responsible for fewer defects in the bulk and on the surface of the drawn films, resulting in less light scattering and hence high clarity. These highly transparent films possess a maximum Young's modulus of 27 GPa and a maximum tensile strength of 800 MPa along the drawing direction, both of which are more than 10 times higher than those of PC and PMMA. Results showed that a wide processing window ranging from 90 °C to 110 °C can be used to tailor the required balance between optical and mechanical performance. It is anticipated that these lightweight, low-cost, highly transparent, high strength and high stiffness HDPE films can be used in laminates and laminated composites, replacing traditional inorganic and polymeric glass for applications in automotive glazing, buildings, windshields, visors, displays etc.

Graphical abstract

Keywords

Polyethylene; Solid-state drawing; Drawing temperature; Transparency; Tensile strength

2

1. Introduction

When it comes to transparent polymeric materials, polycarbonate (PC), poly(methyl methacrylate) (PMMA) and polystyrene (PS) are typically the materials of choice. These plastics have a high optical transparency, with transmittance values of 88−92 % in the visible light regime. Since they are amorphous polymers, the absence of crystalline regions contributes to their optical transparency. However, mechanical properties of these polymers in terms of elastic modulus and tensile strength are relatively unsatisfactory, with values of only 2−3 GPa and 50−70 MPa, respectively [1, 2].

In the case of semi-crystalline polymers like polypropylene (PP) and polyethylene terephthalate (PET), transparent products can be manufactured by controlling polymer morphology, requiring the dimensions of spherulites to be much smaller than the wavelength of visible light. One way to achieve this is by adding nucleating or clarifying agents, as in the case of sorbitol-clarified isotactic PP [3, 4]. Furthermore, transparent amorphous PET products can be acquired by rapid cooling of the melt to below the glass transition temperature (T_g).

High-density polyethylene (HDPE), another type of semi-crystalline polymer, is one of the most commonly used plastics. Approaches for making transparent PP and PET are typically not suitable for making polyethylene products transparent because of a too rapid crystallization rate and low T_g. Typically, HDPE is processed via injection molding or extrusion-based melt processes, leading to isotropic or near isotropic materials and a relatively low elastic modulus (< 1.1 GPa) and tensile strength (< 35 MPa) [5]. Cast or blown film extrusion of HDPE can lead to transparent products [6-10]. However, such materials are often stretched in the melt, meaning that chain entropy and chain relaxation prevents effective chain orientation and chain extension. As a result, mechanical properties of such transparent

HDPE sheets are typically low, with elastic modulus values of 3-4 GPa and tensile strengths of around 100-200 MPa [6-10]. The limited mechanical properties of such extrusion cast or blown polyethylene products restricts their application area mainly to packaging.

Rather than stretching in the melt, a low-cost more effective post-processing method to increase the stiffness and tensile strength of polymeric materials, notably polyolefins, is by uniaxial drawing in the solid-state at temperatures close to but below the melting temperature [11]. For instance, the Young's modulus and tensile strength of ultra-drawn HDPE fibers can be as high as 70 GPa and 1.5 GPa, respectively [12-15]. In the case of ultra-high molecular weight polyethylene (UHMWPE), solid-state drawing is also widely used in combination with solution-processing or solvent-free techniques [16-19]. Here, Young's moduli and tensile strengths have been reported of 100–180 GPa and 2–5 GPa, respectively [20, 21]. Uniaxial drawing in the solid-state is effective in improving mechanical properties of polymers like HDPE because chain relaxation phenomena are limited or absent and hence a high degree of chain orientation and chain extension is generated [22, 23].

Similar to isotropic HDPE products, also solid-state drawn HDPE fibers or films are normally not transparent. For one thing, the dimensions of the crystals, being larger than the wavelength of visible light, and the high degree of crystallinity partially account for the poor transparency [24]. Besides, the introduction of internal voiding and defect structures on the surface and in the bulk of the fibers or films after ultra-drawing will induce light scattering, resulting in a poor transparency in the visible light regime [25]. Hence, resultant opaque oriented polymer products have limited applicability in fields like built environment, visors and automotive glazing where both high transparency and mechanical properties are needed.

In a recent study, Shen *et al.* [26, 27] successfully prepared highly transparent and oriented HDPE films by adding small amounts of specific additives like 2-(2H-benzotriazol-2-yl)-4,6-

ditertpentylphenol (BZT). It was argued that these additives predominantly reduced interfibrillar scattering, resulting in an optical transmittance after drawing of around 90 %. Moreover, these additive-containing ultra-drawn HDPE films possessed a high modulus (~ 18 GPa) and a high tensile strength (~ 650 MPa).

Herein, high transparency and high mechanical performance were simultaneously introduced into HDPE films, simply by regulating the drawing conditions without the need to incorporate additives. The influence of drawing conditions, especially drawing temperature, on optical performance of solid-state drawn HDPE films is systematically explored for the first time. Moreover, the current study further investigates the impact of drawing parameters on drawing behavior, film morphology, mechanical and thermal properties.

2. Experimental

2.1. Materials

Borealis VS4580 (Borealis AG, Austria) was used as high-density polyethylene (HDPE). This polymer grade has a melting temperature (T_m) of 134 °C, a pellet density of 0.958 g/cm^3 and a melt flow index (MFI) of 0.6 g/10 min at 190 °C/2.16 kg and 21 g/10 min at 190 °C/21.6 kg. Clearly, the HDPE grade selected will have a major effect on drawability and ultimate mechanical properties of the films. For example, only homopolymer grades without long chain branching will lead to high draw ratios and mechanical properties. In this study, the HDPE grade selected was based on the seminal work on drawing of HDPE fibers by Ward and coworkers [12, 28, 29], and Wu and Black [14]. They performed a comprehensive study on different grades to achieve ultimate mechanical properties in melt-spun solid-state drawn HDPE fibers. Thermoplastic polyurethane (TPU) ST-6050 sheets were provided by Schweitzer-Mauduit International, Inc. (USA).

2.2. Preparation of Specimens

Isotropic HDPE sheets with a thickness of 0.2–0.5 mm were manufactured by compression molding using a Dr. Collin P300E (Germany) hot press at 160 °C for 3 min, followed by cooling down to room temperature (RT). For optical properties, optical microscopy and thermal characterizations, rectangular-shaped samples with gauge dimensions of 20 mm × 10 mm were cut from these hot-pressed sheets. For surface morphology imaging as well as mechanical tests, dumbbell-shaped specimens were cut from these isotropic sheets according to ASTM D638 Type V with gauge dimensions of 9.5 mm × 3.2 mm. All these samples were then uniaxially drawn at different drawing temperatures from 70 °C to 125 °C in an Instron 5900R84 (UK) universal tensile tester equipped with an environmental chamber. Drawing speed was varied between 100 mm/min to 500 mm/min, although most of the drawing was performed at 100 mm/min. Draw ratio was measured by the length ratios before and after drawing using ink marker lines initially spaced every 1–2 mm. The average thickness (t) of the drawn HDPE samples was calculated by weighing the samples, and using the following equation:

$$t = \frac{m}{\rho \times l \times w} \tag{1}$$

Where m is the mass of the oriented HDPE films, ρ is the density of the oriented films (assuming a crystal density of 1 g/cm^3 based on previous research [26, 30]), and l and w are respectively, the length and width of the films after solid-state drawing. At least three specimens were used for each test.

Specimens for optical appearance and properties as well as optical microscopy consisted of drawn HDPE films sandwiched between TPU interlayers and two glass slides (see *Fig. 2(a)* in Section 3) in order to remove surface scattering from the uniaxially oriented films.

6

Compression molding of this laminated structure was performed using a Rondol (UK) hot press at 100 °C for 5−10 min and a pressure of 3 bar.

2.3. Characterization

Transmittance spectra of the HDPE/TPU/Glass laminates were obtained using a PerkinElmer Lambda 950 (USA) UV-vis spectrometer equipped with an integrating sphere with 100 mm diameter in the wavelength range of 400−700 nm at an interval of 1 nm, measured at least three times for each sample. UV-vis tests were carried out at a sample-to-detector distance of 5 cm and 40 cm (see schematic diagrams in *Fig. 4(a)* and *4(b)* in Section 3). Optical microscopy of laminates was performed using an Olympus BX60 (USA) microscope in transmission-mode. The percentage of area coverage by microvoids in the drawn HDPE films was calculated from optical microscopy images using ImageJ software.

Atomic force microscopy (AFM) images of drawn HDPE films were taken using a NT-MDT NTEGRA (Russia) system with a Mikromasch probe. The probe had a resonant frequency of around 160 kHz and a spring constant of 5 N/m. The AFM images were captured at a frequency of 0.5−1 Hz and a set point ratio of 2.0. The surface roughness of drawn HDPE films was calculated from the AFM images by SPIP software analysis. Scanning electron microscopy (SEM) of drawn HDPE films was carried out using FEI Inspect F (Netherlands) with an acceleration voltage of 5 kV.

Differential scanning calorimetry (DSC) of drawn HDPE films was carried out using a TA Instruments (UK) DSC25. Samples of 5−10 mg were placed in aluminum pans with a single heating-cooling cycle performed under a flow of nitrogen gas at a constant heating rate of 10 °C/min. At least three tests were carried out for each condition. The melting point (T_m) and enthalpy of fusion (ΔH_f) of the drawn films were obtained from the first heating scan. The crystallinity (X_c) was calculated using the following equation:

$$X_c = \frac{\Delta H_f}{\Delta H_f^0} \times 100\ \% \tag{2}$$

Where ΔH_f^0 is the enthalpy of fusion of 100 % crystalline polyethylene crystals, which is equal to 293.0 J/g [31].

The maximum draw ratio which still produced transparent films was judged by visual inspection during the solid-state drawing process. Above a specific draw ratio, whitening occurred in the drawn films. The maximum transparent draw ratio (λ_{trans}) was defined at this critical point, which was different from the maximum draw ratio (λ_{max}) which was defined as the draw ratio at break. Young's modulus and tensile strength of drawn oriented HDPE films were measured using an Instron 5566K1071 (UK) universal tensile tester at a crosshead speed of 100 mm/min at RT. Specimens with gauge lengths of 50–100 mm were tested using manual wedge action grips. Young's modulus was calculated from the tangent of the engineering stress-strain curve at a strain below 0.5 %. The mean and standard deviation of the Young's modulus and tensile strength were calculated from at least three samples.

3. Results and discussion

The engineering stress-strain curves of HDPE films during solid-state drawing at different drawing temperatures (T_d) are shown in *Fig. 1(a)*. With increasing drawing temperature, the yield stress significantly drops from 13.8 MPa to 3.6 MPa for drawing temperatures ranging from 70 °C to 120 °C. Also, strain hardening behavior becomes less pronounced with increasing drawing temperatures. At $T_d \leq 110$ °C, strain hardening results in stable neck formation and homogeneous deformation even at high draw ratios (λ). However, the solid-state drawing process becomes inhomogeneous with localized necking at low draw ratios when $T_d > 110$ °C as a result of the weak strain hardening. In fact, heterogeneous drawing

with highly deformed regions and close to non-deformed regions were always observed under these conditions and consequently proper and reproducible samples were difficult to obtain due to the lack of strain hardening. *Fig. 1(b)* shows the maximum draw ratio (λ_{max}) and the maximum transparent draw ratio (λ_{trans}) as a function of drawing temperature, where λ_{max} is related to the maximum extensibility of the molecular network above which further drawing would lead to failure i.e., no further orientation would develop, whereas λ_{trans} is the maximum draw ratio before 'whitening' starts to occur and the film becomes opaque. At $T_d = 80$ °C, the highest λ_{max} is obtained for this grade of HDPE, indicating an optimum drawing temperature of 80 °C for ultimate mechanical performance. Similar optimum drawing temperatures for ultimate mechanical properties of oriented HDPE were also reported by both Jarecki and Meier [32] and Capaccio *et al.* [28]. However, all uniaxially oriented films are opaque at $T_d \leq$ 80 °C. Conversely, transparent films are obtained at $T_d \geq 90$ °C. Both λ_{max} and λ_{trans} are reduced with further increasing drawing temperatures due to less strain hardening. Hence, transparent oriented HDPE films and homogeneous drawing even at high draw ratios were obtained in a temperature window between 90 °C and 110 °C.
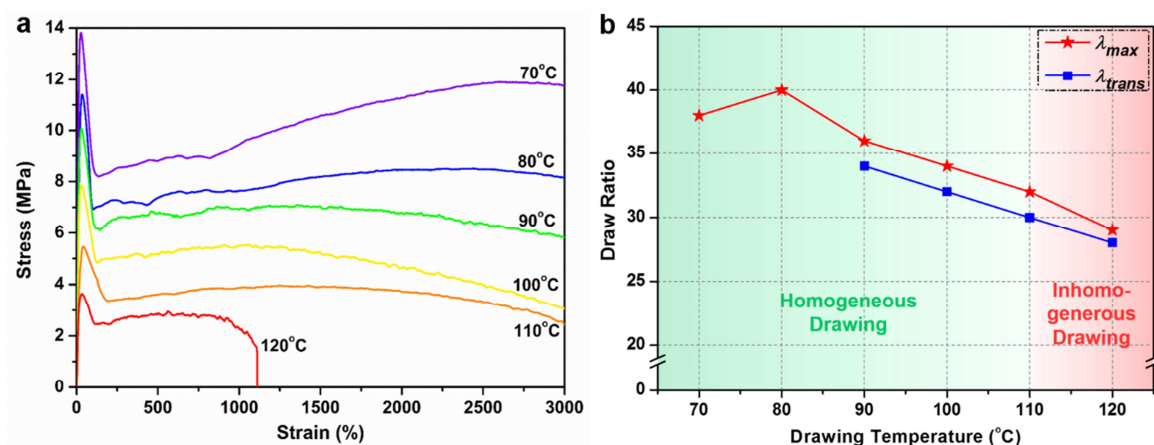

9

Fig. 1. (a) Stress-strain curves at different drawing temperatures and (b) λ_{max} and λ_{trans} of oriented HDPE films as a function of drawing temperature at a drawing speed of 100 mm/min. The background color change from green to red signifies the transition from homogeneous to inhomogeneous drawing and indicates the processing window for creating highly oriented polymer films.

Besides drawing temperature, the drawing speed also influences the solid-state drawing process of HDPE films. Both the yield stress and strain hardening increases with increasing drawing speed (see Supporting Information *Fig. S1(a)*). As a result of this increase in strain hardening, drawing behavior becomes more stable, leading to an increase in λ_{max} and λ_{trans} with drawing speed (see *Fig. S1(b)*). In accordance with time-temperature equivalence [33] this trend is opposite to that of drawing temperature (*Fig. 1(a)* and *1(b)*).

In order to remove the influence of surface scattering when evaluating the optical properties of uniaxially oriented HDPE films, these films were sandwiched between two glass slides with TPU interlayers as schematically shown in *Fig. 2(a)*. The chosen TPU interlayers have a refractive index ($n = 1.50$) similar to glass ($n = 1.52$) [34] and HDPE ($n = 1.54$) [5], reducing the degree of light reflections at the interfaces. After being sandwiched between glass and TPU, a more clear appearance with higher transmittance values is observed for the oriented HDPE films (*Fig. 2(b)* and *2(c)*), which means that the TPU interlayers successfully eliminate the light scattering at the surface of the HDPE films. The thickness of the films also affects their optical performance. Thinner films usually possess higher transparency (*Fig. S2*) since they contain fewer defects or dust particles that can scatter light. HDPE films with a thickness of ~275 μm after drawing (shown as the blue line in *Fig. S2*) were drawn from compression-molded films with a thickness of around 1 mm. These films still possessed a

transmittance of ~81 % at 550 nm. However, above this thickness, with the current set-up it became hard to carry out the solid-state drawing process.
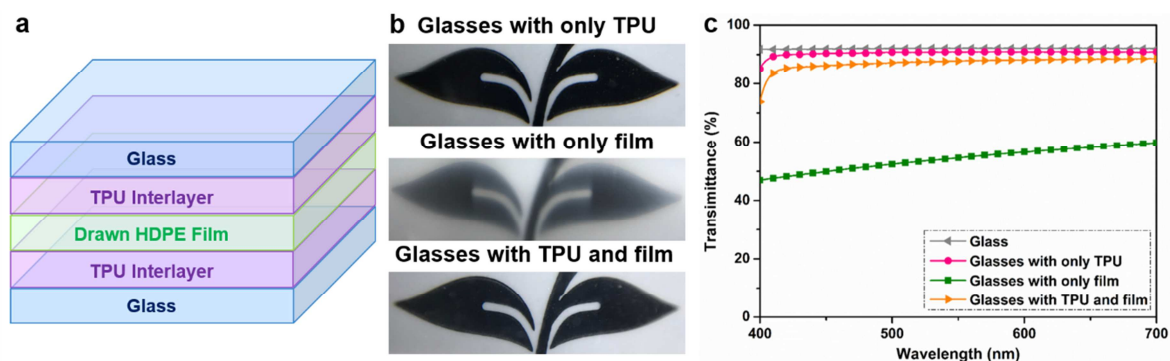

Fig. 2. (a) Schematic diagram of the laminated structure consisting of drawn HDPE film sandwiched between glass slides and TPU interlayers, (b) photographs and (c) transmittance of glass, TPU interlayers sandwiched between two glass slides, drawn HDPE films sandwiched between two glass slides with or without TPU interlayers versus visible light wavelength tested at a sample-to-detector distance of 40 cm.

Nearly all studies in the literature that are concerned with optical transparency use photographs of sample appearances by positioning the sample at a very close distance to an object, often involving placing the "transparent" sample directly on top of a background image [4, 35, 36]. However, according to ASTM D1746-15, regular transmittance usually refers to the ability of an observer to "see-through" a specimen in order to clearly distinguish a relatively distant object, analogous to the visibility of the distant scenery seen through a window. Here, the optical appearance of the oriented HDPE films ($\lambda = 15$) drawn at different temperatures is shown when placed close to an object but also at a relatively far distance from an object (***Fig. 3***). It is shown that the drawn films are completely opaque at $T_d = 70\ ^\circ\text{C}$ and $80\ ^\circ\text{C}$. However, when the drawing temperature is increased from $80\ ^\circ\text{C}$ to $90\ ^\circ\text{C}$, the appearance of the drawn HDPE films changes from opaque to transparent. Films drawn above $100\ ^\circ\text{C}$ have a highly transparent appearance with little differences in optical

appearance. Moreover, the visibility as seen through opaque films (T_d = 70 °C and 80 °C) or translucent films (T_d = 85 °C) when placed at a far distance from an object (**Fig. 3(b)**) is less than when placed close to an object (**Fig. 3(a)**). It is noteworthy that in the case of translucent films drawn at 85 °C, an object is still slightly visible when the HDPE film is placed close to the object, whereas it is not at all visible when the film is placed at a distance. This once more highlights the importance of evaluating transparency not only at a short sample-to-object distance (near field) but also at a long sample-to-object distance (far field).
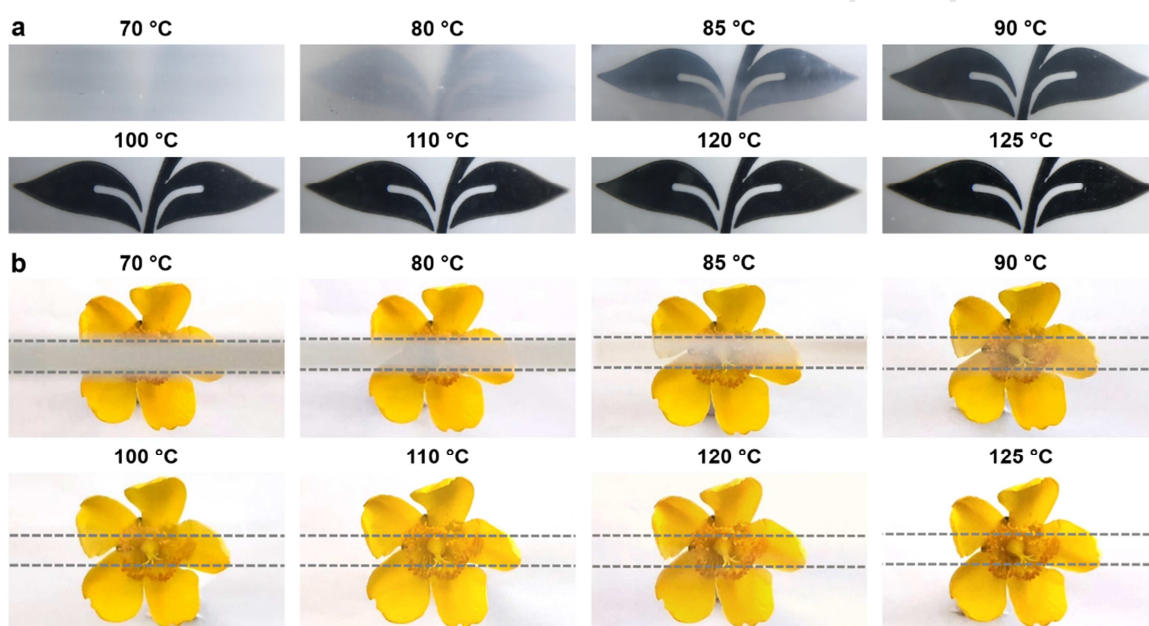

Fig. 3. Photographs of oriented HDPE films (λ = 15) drawn at different drawing temperatures (a) when placed directly on top of an object (near field) and (b) when placed at a 40 cm distance from an object (far field). HDPE films were sandwiched between glass slides and TPU interlayers. In (b), the films are marked and located between the dashed lines. The thickness of the drawn HDPE films is around 80 µm.

Similarly, also transmittance spectra for solid materials are customarily measured in the near field using a short sample-to-detector distance (typically below 5 cm) in a UV-vis machine [37, 38]. Here, optical performance was tested at both a short (near field) and a

relatively long sample-to-detector distance (far field). For a sample-to-detector distance of 5 cm, the sample was placed at the entrance port of the integrating sphere (***Fig. 4(a)***). In this case the transmittance spectra contain the light scattered in the forward direction. At a sample-to-detector distance of 40 cm, the specimen was placed further away from the integrating sphere which gives more relevant transmittance data (***Fig. 4(b)***). Transmittance spectra at both sample-to-detector distances are shown in ***Fig. 4(c)*** and ***4(d)***. Transmittance values measured at both distances are around 92.0 % for glass and 90.5 % for a single TPU interlayer sandwiched between two glass slides. For HDPE film drawn at 110 °C sandwiched between two glass slides and TPU interlayers, the transmittance at 40 cm sample-to-detector distance is 1–2 % lower than the value measured at a distance of 5 cm. However, differences in transmittance as high as 16 % or 28 % are obtained at these two distances for HDPE films drawn at 85 °C or 80 °C, respectively. This discrepancy in transmittance values for different sample-to-detector distances is in accordance with the optical appearance at different sample-to-object distances (see ***Fig. 3(a)*** and ***3(b)***). Bearing in mind potential practical applications for transparent high strength HDPE films, subsequent optical tests were all performed at a sample-to-detector distance of 40 cm (far field).
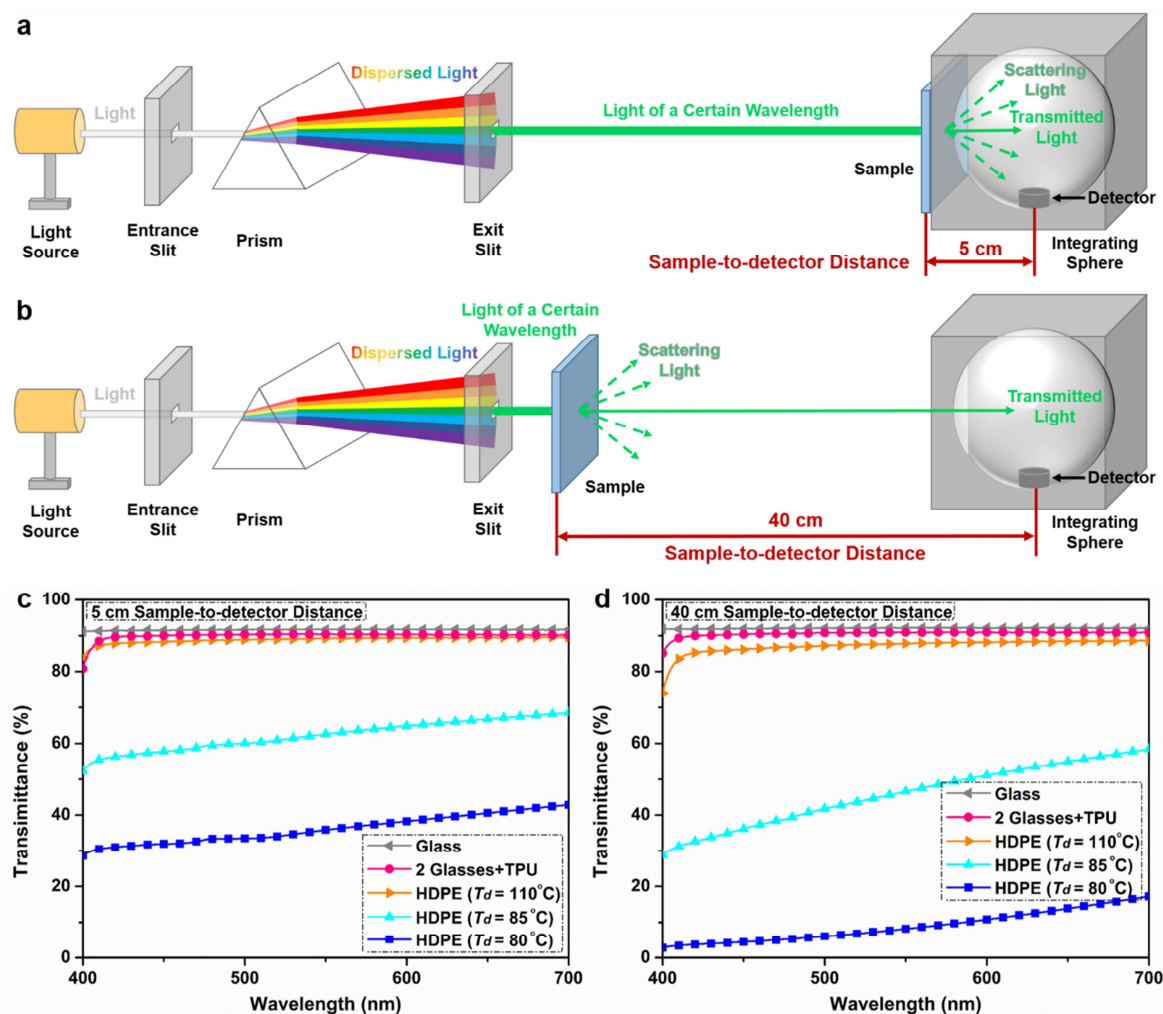
Fig. 4. Schematic diagrams of the beam path inside the UV-vis machine, corresponding to two different sample-to-detector distances of (a) 5 cm and (b) 40 cm together with transmittance data versus wavelength tested at a sample-to-detector distance of (c) 5 cm and (d) 40 cm. Drawn HDPE films ($\lambda = 15$) were sandwiched between glass slides and TPU interlayers.

The influence of drawing temperature on transmittance in the visible light range is shown in **Table 1** and **Fig. 5(a)**. At $T_d \leq 80$ °C, transmittance values of drawn HDPE films at $\lambda = 15$ are all below 18 %. Transmittance of the uniaxially oriented films increases to over 75 % when T_d increases to 90 °C. More importantly, with further increasing drawing temperatures ($T_d \geq$ 100 °C), optical transmittance can exceed 89 % at high wavelengths within the visible

spectrum, which is only 3 % lower than glass (~ 92 %). Higher chain mobility resulting in fewer defects at elevated drawing temperatures may account for this increase in transparency. However, as illustrated in *Fig. S3*, transmittance values also gradually decrease with increasing drawing speed at similar draw ratio. Accordingly, an optimized combination of drawing temperature and drawing speed should be aimed for when requiring high optical clarity.

Table 1. Transmittance values of drawn HDPE films (λ = 15) at different drawing temperatures at a wavelength of 700 nm, 550 nm and 400 nm measured at a sample-to-detector distance of 40 cm.

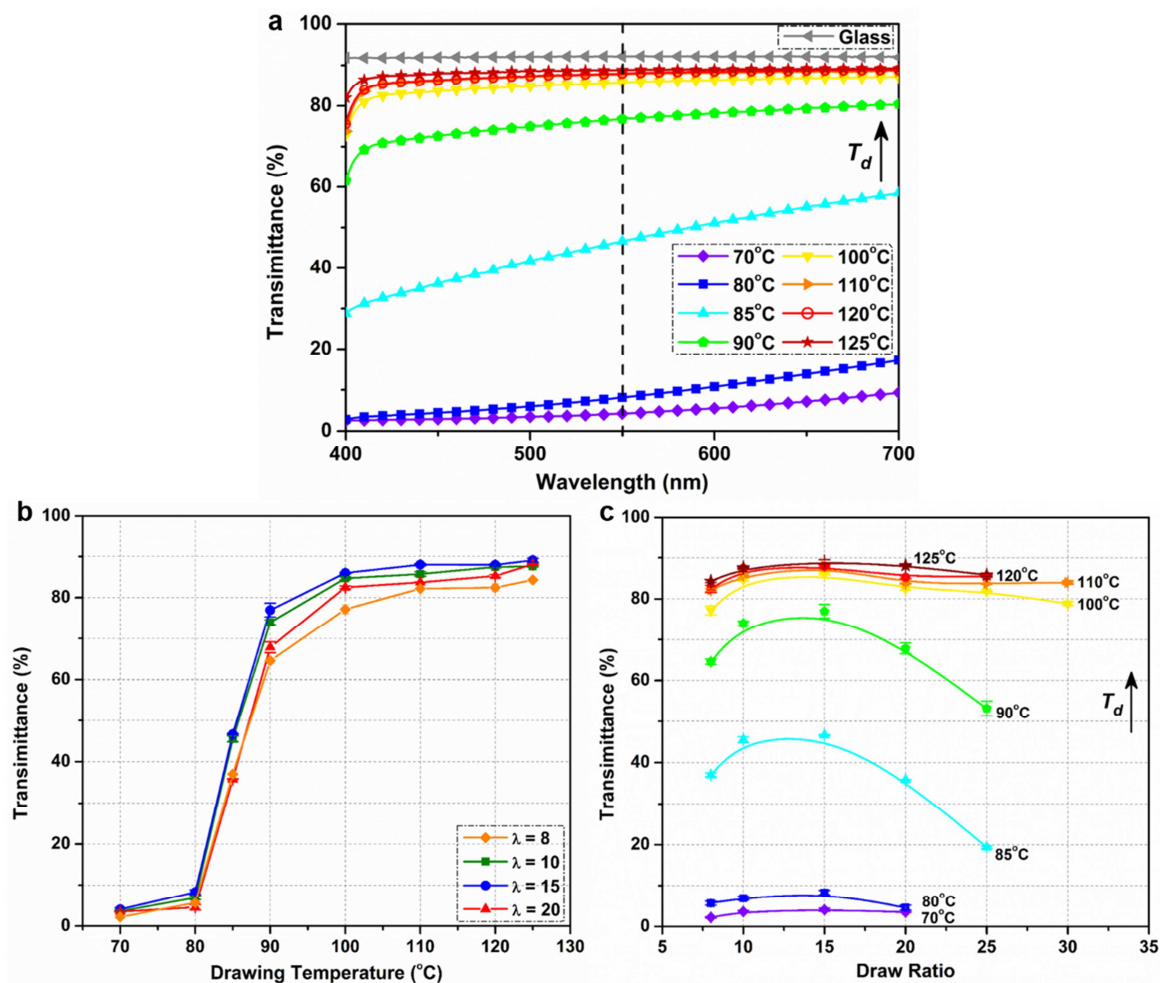| Wavelength	70 °C	80 °C	85 °C	90 °C	100 °C	110 °C	120 °C	125 °C
700 nm	9.3 %	17.2 %	58.5 %	80.5 %	87.1 %	88.5 %	88.9 %	89.2 %
550 nm	4.3 %	8.2 %	46.6 %	76.7 %	85.8 %	87.8 %	88.0 %	88.9 %
400 nm	2.5 %	2.8 %	28.8 %	61.5 %	73.1 %	73.8 %	75.5 %	82.0 %

Fig. 5. Transmittance of drawn HDPE films (a) at $\lambda = 15$ at different drawing temperatures versus visible light wavelength, (b) at different draw ratios as a function of drawing temperature and (c) at different drawing temperatures as a function of draw ratio at a wavelength of 550 nm, indicating maximum transmittance at $T_d \geq 100$ °C and $\lambda = 15$. Drawn HDPE films were sandwiched between glass slides and TPU interlayers and tested at a sample-to-detector distance of 40 cm. The thickness of the drawn HDPE films is about 80 µm.

It is well known that the most sensitive wavelength to the human eye is around 550 nm within the visible spectrum. *Fig. 5(b)* gives the change in transmittance with increasing drawing temperature at this wavelength. Transmittance of drawn HDPE films at $\lambda = 15$ is significantly improved within the T_d range of 80−90 °C. Transmittance becomes even better (≥ 86 %) for $T_d \geq 100$ °C, with films showing a consistent tendency of improved optical clarity with increasing drawing temperature.

Fig. 5(c) further demonstrates the influence of draw ratio on optical transparency of drawn HDPE films. It is shown that for all drawing temperatures, transmittance is maximum at around $\lambda = 15$, with transmittance decreasing at higher draw ratios. The initial increase in transmittance is most likely related to the change in polymer morphology from an isotropic spherulitic structure to an oriented structure [39]. The slight decrease in optical properties at high draw ratios can be attributed to the formation of defects in a highly fibrillar structure, leading to light scattering. The observation of an optimum draw ratio for high transparency is in accordance with previous research in the area of transparent HDPE films using additives to enhance transparency [26]. Another remarkable observation is that transmittance values of drawn HDPE films show only little improvement for $T_d \geq 100$ °C for each draw ratio, indicating that a plateau in optical transparency is reached around this temperature.

The outcomes of these optical experiments indicate that by simply raising the drawing temperature in the solid-state drawing process, transparency of oriented HDPE films can be significantly enhanced. For the purpose of exploring the mechanism behind this improvement in transmittance with increasing drawing temperatures, optical microscopy images of drawn HDPE films at different T_d were taken (*Fig. 6*). It can be seen that a number of parallel interfibrillar microvoids along the drawing direction are present in films drawn at 70 °C and 80 °C. As a result, less light can penetrate through these films due to light scattering effects by these microvoids which contributes to the darkened images. When T_d is raised to 90 °C,

17

the amount of parallel interfibrillar microvoids clearly diminishes. The area covered by these parallel microvoids as quantified by ImageJ software drops from 42.7 % at $T_d = 80$ °C to 4.2 % at $T_d = 90$ °C. This implies that more light can pass through films produced at $T_d = 90$ °C because less light is scattered, resulting in a much brighter image. The number of interfibrillar microvoids is even further reduced for $T_d \geq 100$ °C, with only 0.1 % coverage by parallel microvoids at $T_d = 120$ °C. This is consistent with the highly transparent appearance and high transmittance values of films drawn at high temperatures (see *Fig. 3* and *5*).
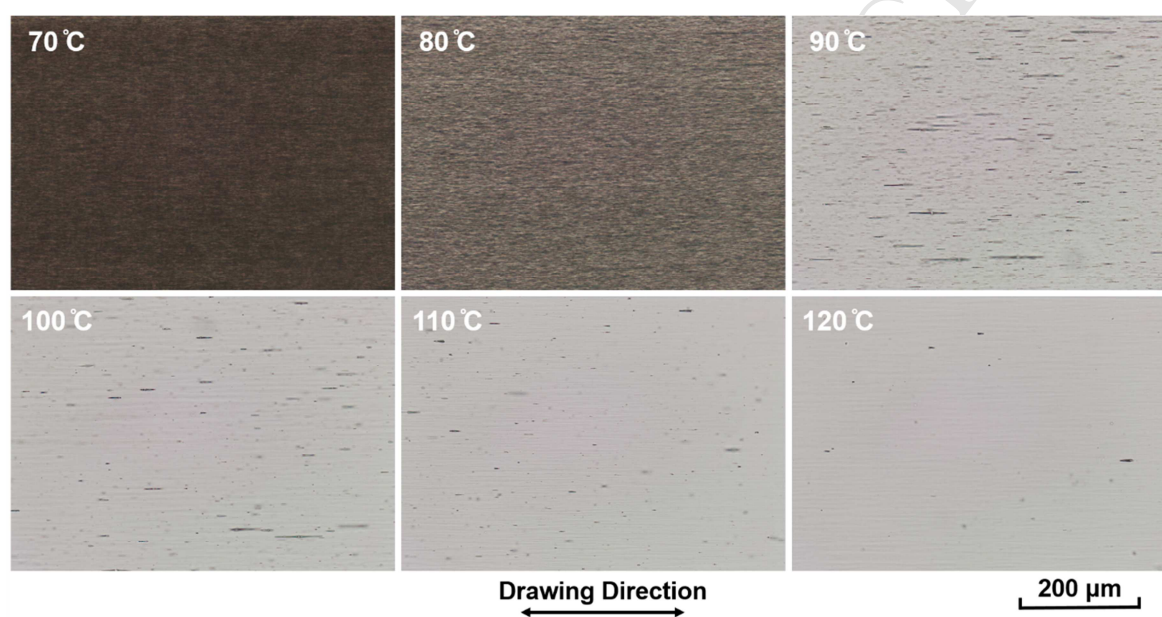

Fig. 6. Optical microscopy images of drawn HDPE films ($\lambda = 15$) at different drawing temperatures taken at the same light intensity in the optical microscope, showing a reduction in parallel microvoids with increasing drawing temperature. Drawn HDPE films were sandwiched between glass slides and TPU interlayers.

AFM images in *Fig. 7* reveal the surface structure of drawn HDPE films ($\lambda = 15$) at a drawing temperature of 80 °C and 110 °C. The films drawn at $T_d = 80$ °C display obvious fibrillar and wrinkled surface structures (*Fig. 7(a)*), with an average surface roughness (*Sa*) of 118 nm. According to Peterlin's molecular model of the drawing of polyolefins [39, 40],

18

the morphology of semi-crystalline polymers will change from a spherulitic structure to a newly generated fibrillar structure during drawing. In comparison, films drawn at $T_d = 110$ °C reveal a smoother surface structure (***Fig. 7(b)***) with a lower average surface roughness (*Sa*) of 89 nm. We think that this reduction in surface roughness at high drawing temperatures is the result of higher chain mobility and relaxation at these elevated temperatures [41, 42].
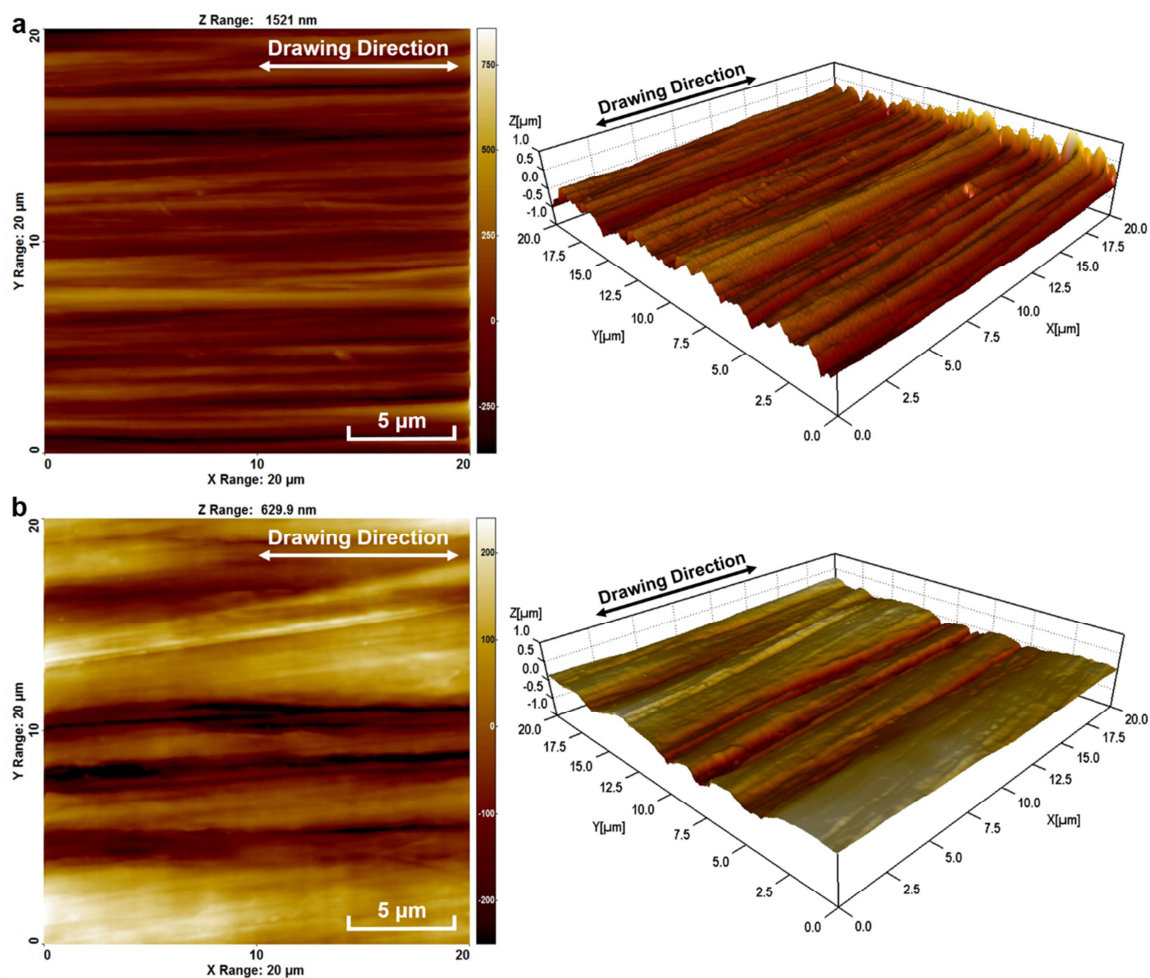

Fig. 7. 2D and 3D AFM images of drawn HDPE films ($\lambda = 15$) drawn at (a) $T_d = 80$ °C and (b) $T_d = 110$ °C, showing a smoother surface morphology at higher drawing temperature.

SEM images (***Fig. 8***) further reveal the change in surface morphology of HDPE films ($\lambda = 15$) drawn at 70−120 °C. With increasing drawing temperatures, the fibrillar microstructure with fibrils along the drawing direction appears less pronounced and the width of the fibrils

broadens. We believe that higher drawing temperatures will give rise to relaxation of oriented chains, facilitating the mobility of polymer chains as well as reducing the separation of fibrils in drawn HDPE films [25]. The decreasing number of interfibrillar voids then contributes to reduced interfibrillar scattering, and hence enhanced transparency together with an optically clear appearance at higher drawing temperatures.
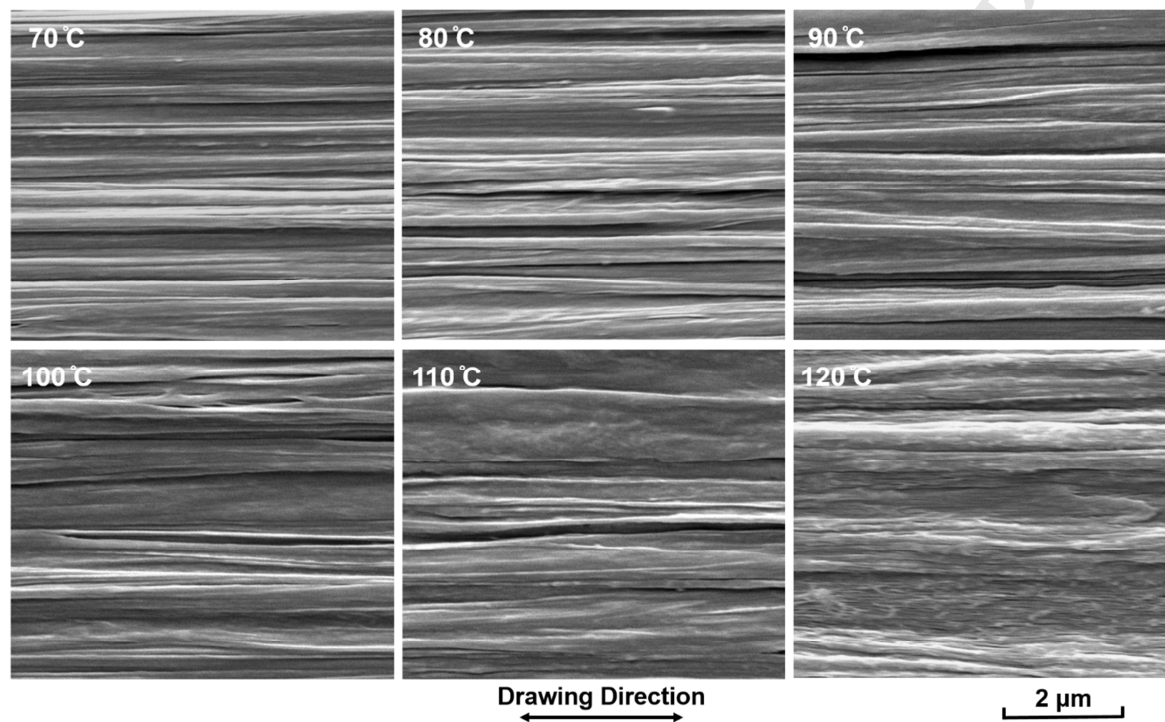

Fig. 8. SEM images of drawn HDPE films ($\lambda = 15$) at different drawing temperatures, showing less interfibrillar defects with increasing temperature.

In terms of thermal properties, the melting temperatures (T_m) of drawn HDPE films fluctuate at around 141 °C for $T_d = 70{-}125$ °C and therefore T_m can be regarded as independent of drawing temperature for a draw ratio of 15 (see **Fig. S4(a)**). It signifies that drawing temperature has limited impact on thermal properties of drawn HDPE films at this draw ratio, which is in agreement with previous studies [32]. However, crystallinity (X_c) did slightly increase (~ 5 %) with increasing T_d.

To further investigate the effect of draw ratio on films' optical performance, optical microscopy and SEM images of drawn HDPE films with different draw ratios at $T_d = 110$ °C are shown in *Fig. 9* and *10*, respectively. It is found that the number of microvoids parallel to the drawing direction increases markedly above $\lambda = 20$ (see *Fig. 9*), with 0.4 % area coverage by parallel microvoids at $\lambda = 15$ and 1.5 % coverage at $\lambda = 30$. The increase in parallel microvoids explains the reduced transparency for drawn HDPE films of high draw ratios ($\lambda >$ 15) because of the induced interfibrillar light scattering. Similar changes in transparency at high draw ratios were also observed in solid-state drawn polypropylene (PP) tapes [43] and poly(lactic acid) (PLA) tapes [44]. Furthermore, significant microcracking perpendicular to the drawing direction (indicated by the circles in *Fig. 10*) can be seen in SEM images at $\lambda \geq$ 20, which may also lead to severe light scattering inside the films and hence a decrease in transparency. Similar perpendicular cracking and associated changes in appearance from transparent to opaque were also observed by Schimanski *et al.* [43] for PP. These perpendicular microcracks, which are often associated with overdrawing, also restrict further deformation and orientation of molecular chains, resulting in a trend of decreasing λ_{max} and λ_{trans} above $T_d = 80$ °C (see *Fig. 1(b)*). Microvoids along the drawing direction occur at relatively low drawing temperatures or at relatively high draw ratios and are predominately present in the bulk of the oriented films [26]. Hence, they hardly present in SEM images (*Fig. 8* and *Fig. 10*) but do show in optical microscopy images under transmission-mode (*Fig. 6* and *Fig. 9*). In conclusion, microvoiding both along and perpendicular to the drawing direction of the polymer films induced at relatively low drawing temperatures ($T_d \leq 80$ °C) or high draw ratios ($\lambda \geq 20$) will increase the amount of light scattering inside the drawn HDPE films, hence leading to a deterioration in transparency. With respect to thermal properties, both T_m and X_c gradually increase with increasing λ. In *Fig. S4(b)*, the increase in T_m and X_c between HDPE films ($\lambda = 30$) drawn at 110 °C and the original isotropic hot-pressed film is

shown to be 5 °C and 12.5 %, respectively. Based on previous studies [45, 46], this can be explained by orientation of the amorphous phase during drawing, leading to an increase in density of the amorphous region. As a result, chain relaxation is hindered by the dense chain packing and taut tie molecules during heating, and consequently results in the increase of T_m and X_c.
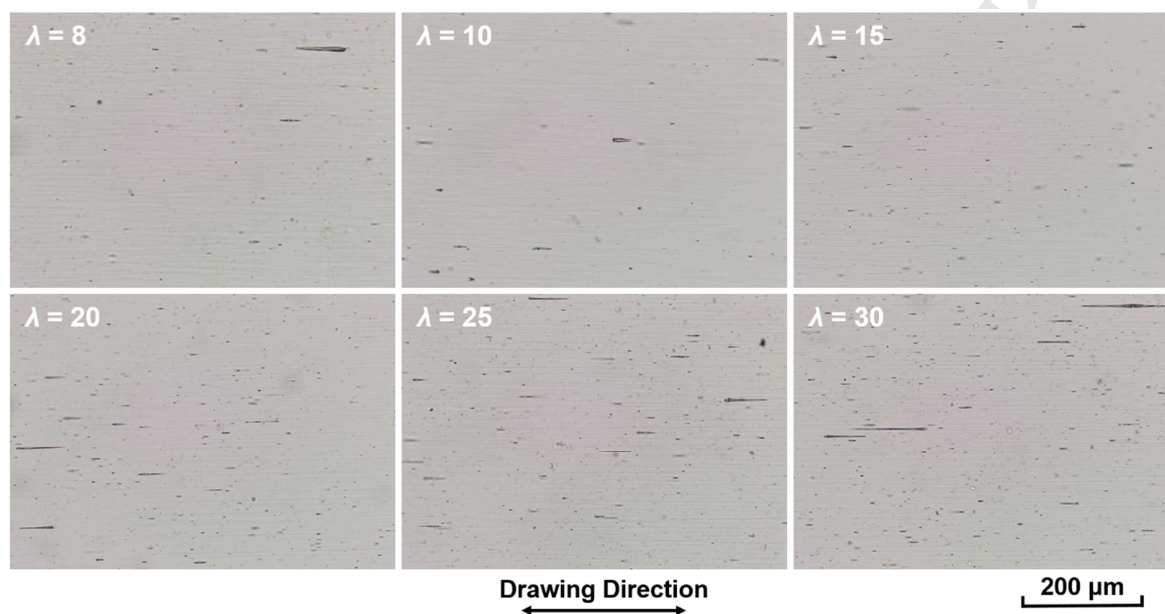

Fig. 9. Optical microscopy images of drawn HDPE films with different draw ratios at $T_d =$ 110 °C taken at the same light intensity in the optical microscope, showing an increase in parallel microvoids at high draw ratios. Drawn HDPE films were sandwiched between glass slides and TPU interlayers.
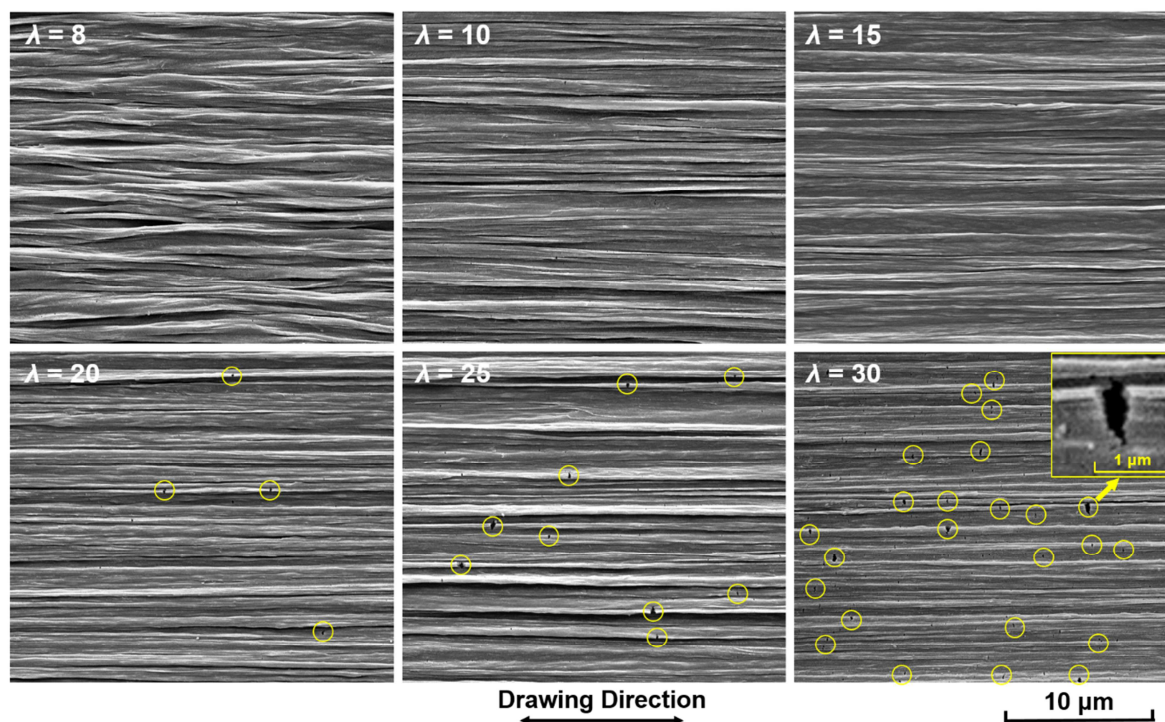
Fig. 10. SEM images of HDPE films drawn at $T_d = 110$ °C at different draw ratios, showing a clear increase in defects at high draw ratios. The circles mark the microcracking defects perpendicular to the drawing direction. The inset in the image for $\lambda = 30$ shows a higher magnification image of this type of microcracking defect.

The Young's modulus and tensile strength of drawn HDPE films along the drawing direction are shown in **Fig. 11** at different drawing temperatures and draw ratios. First, with increasing draw ratio, elastic modulus and tensile strength along the drawing direction are improved as a result of the unfolding of molecular lamellae and high degree of chain orientation induced by solid-state drawing. Young's modulus is independent of drawing temperature for $T_d \leq 100$ °C and draw ratios between 10 and 20 (**Fig. 11(a)**), with modulus values of around 19 GPa for drawn HDPE films at the highest transparent draw ratio ($\lambda = 15$). Moreover, a modulus of around 27 GPa can be achieved for drawn HDPE films at $\lambda = 20$ and $T_d = 80–100$ °C owing to the formation of taut tie molecules induced by the deformation and orientation of polymer chains in the drawn films [39]. These well-oriented tie molecules effectively connect

23

crystalline regions and therefore contribute to a high modulus. For drawing temperatures below 100 °C, the tensile strength is about 650 MPa and 800 MPa at $\lambda = 15$ and $\lambda = 20$, respectively (***Fig. 11(b)***). Nevertheless, both modulus and strength drop with increasing T_d above 100 °C at high draw ratios, with values of around 24 GPa and 700 MPa for $\lambda = 20$ at T_d = 110 °C, respectively. This decrease in modulus and strength along the drawing direction is the result of a higher degree of molecular chain relaxation at higher drawing temperatures, and therefore a reduction in the number of taut tie molecules and degree of molecular chain orientation. In addition, the development of parallel microvoids and perpendicular microcracks at high draw ratios can also contribute to this reduction in properties [25, 32] (see ***Fig. 9*** and ***10***). Uniaxially oriented polyethylene films and fibers are highly anisotropic and mechanical properties of ultra-drawn polyethylene films perpendicular to the drawing direction are typically low. As measured in some of our earlier work [47], the Young's modulus and tensile strength perpendicular to the drawing direction of polyethylene tapes with a draw ratio of 20 is around 2 GPa and 15 MPa, respectively. Our drawn HDPE films (λ = 20) are expected to have similar values of modulus and strength in transverse direction.

Clearly, depending on the required performance, an optimum combination of optical and mechanical performance can be obtained after carefully tuning draw ratio and drawing temperature. For instance, if high mechanical performance is preferred, a draw ratio of 20 should be used, yielding a much higher modulus and strength at similar optical transparency (see ***Fig. 5(c)***). Thus, depending on specific applications, transparent and high strength HDPE films can be achieved within a wide processing window for solid-state drawing between 90 °C and 110 °C.
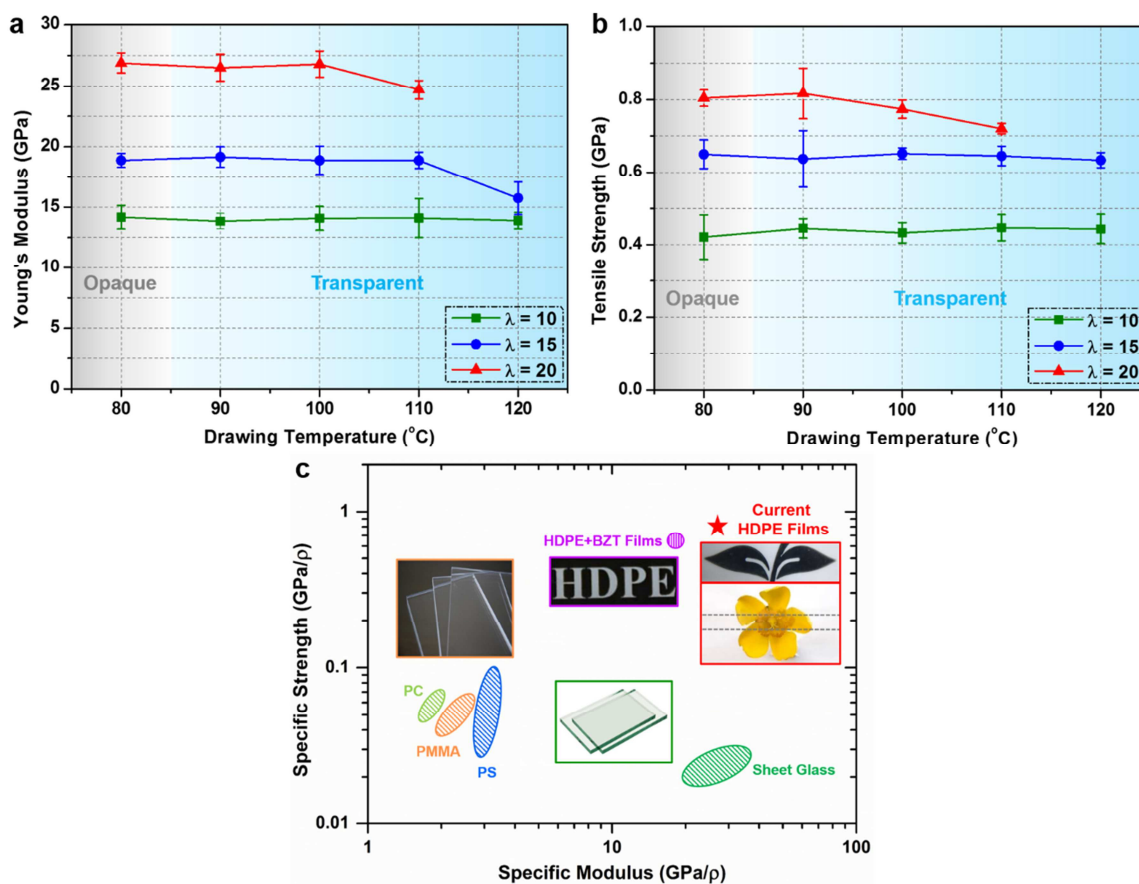
Fig. 11. (a) Young's modulus and (b) tensile strength of drawn HDPE films along the drawing direction at different draw ratios as a function of drawing temperature. (c) Comparison of specific strength, specific modulus and the appearance of common transparent materials together with previous transparent HDPE films with BZT additives [26] and our solid-state oriented HDPE films along the drawing direction. The background color change from grey to blue indicates the transition from opaque to transparent films.

A major advantage of polyethylene over most other solid materials is their low density ($\rho \approx 1$ g/cm^3), which leads to high values of specific strength (tensile strength divided by density) and specific modulus (elastic modulus divided by density) of ultra-drawn polyethylene fibers and films. The specific strength and modulus of our transparent HDPE films along the drawing direction are as high as 800 MPa/g·cm^{-3} and 27 GPa/g·cm^{-3} and are similar to values

for high strength glass fibers. The specific modulus of the transparent films is also similar to that of a classic engineering material like aluminum, while its specific strength is about 7 times higher as aluminum. The specific strength and modulus of common transparent materials like sheet glass, PMMA, PC and PS, drawn HDPE films with BZT additives produced by Shen *et al.* [26] together with our current transparent solid-state drawn HDPE films along the drawing direction produced by tuning drawing temperature are shown in *Fig. 11(c)*. Sheet glass including laminated glass, tempered glass or toughened glass like Gorilla[®] glass has a relatively low specific strength due to its high density ($\rho \approx 2.5$ g/cm^3). In comparison, polymers usually have lower densities around 1–1.5 g/cm^3. Commercial transparent polymeric materials such as PMMA, PC and PS typically possess specific moduli of around 2–3 GPa/g·cm^{-3} and specific strengths of 40–60 MPa/g·cm^{-3}. However, our highly transparent solid-state drawn HDPE films have a specific strength which is more than 10 times higher than both traditional sheet glass and traditional transparent polymeric materials, and also about 20 % higher than previous drawn HDPE films where transparency was induced through the addition of additives like BZT. Hence, our optimized solid-state drawn HDPE films successfully combine high transparency with lightweight, high strength and high stiffness, making them of interest for a wide range of applications. Potential applications of these high strength polymer films and their composite laminates reside in automotive glazing, windshields, displays for electronic devices, glazing for buildings, protective windows, visors and so on. Moreover, such oriented films or tapes could form the basis for a whole new range of transparent 'self-reinforced' or 'all-polymer' composites [48-51].

Apart from drawing parameters such as drawing temperatures, draw ratios and drawing speeds, other factors including molecular weight, molecular weight distribution, long chain branching and crystal characteristics (e.g. lamellar thickness and cell parameters) will also have a remarkable influence on transparency, drawing behavior and ultimate mechanical

performance of the drawn HDPE films [12, 25, 29, 32, 52]. Further research should place more emphasis on these aspects. Moreover, in future the manufacturing of the HDPE films should also be carried out using more industrially relevant processes such as cast film extrusion and in-line drawing. This is the topic of a future paper and includes the effect of shearing and pre-orientation of the melt prior to drawing on ultimate drawability, optical and mechanical properties [53].

4. Conclusions

Transparent, glass-like HDPE films with outstanding mechanical properties were successfully prepared by solid-state drawing at elevated temperatures without the need of additives. The underlying mechanism and the effect of various parameters were systematically explored. HDPE films drawn at $T_d \geq 90$ °C had a transparent appearance, with a maximum transmittance of nearly 90 % at higher drawing temperatures. Increasing drawing temperatures led to higher transmittance values, however at the expense of mechanical properties, resulting in a practical drawing temperature window for transparent high strength HDPE films of 90–110 °C. Optical transmittance of the solid-state drawn HDPE films was optimum for a draw ratio (λ) of 15. Morphological observations revealed a reduction in microvoids parallel to the drawing direction with increasing drawing temperature most likely due to greater chain mobility and the formation of less interfibrillar defects. Microcracking perpendicular to the drawing direction was observed after ultra-drawing ($\lambda \geq 20$), leading to severe light scattering and reduced transparency in these highly fibrillar structures. At a drawing temperature of 90 °C and 100 °C, transparent solid-state drawn HDPE films ($\lambda = 20$) exhibited excellent mechanical properties with a maximum Young's modulus of 27 GPa and a maximum tensile strength of 800 MPa along the drawing direction. Thus, through carefully

controlling drawing parameters, especially drawing temperature and draw ratio, highly oriented HDPE films could be obtained with high levels of optical clarity without the need for additives combined with mechanical properties which are more than 10 times greater than those of common transparent polymers like PC, PMMA and PS. Such transparent solid-state drawn HDPE films and further fabricated laminated composites can potentially replace traditional laminated glass as well as commercial transparent polymeric materials, and are therefore of interest for a wide range of applications including windows and glazing, windshields, visors, displays etc.

Conflict of interest

The authors declare no competing interests.

Acknowledgement

References

[1] C.A. Harper, E.M. Petrie, Plastics materials and processes: a concise encyclopedia, John Wiley & Sons, 2003.

[2] A. Peacock, Handbook of polyethylene: structures, properties, and applications, CRC Press, 2000.

[3] K. Hamada, H. Uchiyama, Polyolefin plastic compositions, US4016118, 1977.

[4] M. Kristiansen, M. Werner, T. Tervoort, P. Smith, M. Blomenhofer, H.-W. Schmidt, The binary system isotactic polypropylene/bis(3,4-dimethylbenzylidene)sorbitol: phase behavior, nucleation, and optical properties, Macromolecules, 36(14) (2003) 5150-5156.

[5] C. Vasile, M. Pascu, Practical guide to polyethylene, iSmithers Rapra Publishing, 2005.

[6] M. Nakamura, S. Yamamoto, Manufacture of polyolefin sheet, JP10323892, 1998.

[7] M.B. Johnson, G.L. Wilkes, A.M. Sukhadia, D.C. Rohlfing, Optical properties of blown and cast polyethylene films: Surface versus bulk structural considerations, J. Appl. Polym. Sci., 77(13) (2000) 2845-2864.

[8] Z. Jiang, Y. Tang, J. Rieger, H.-F. Enderle, D. Lilge, S.V. Roth, R. Gehrke, Z. Wu, Z. Li, X. Li, Y. Men, Structural evolution of melt-drawn transparent high-density polyethylene during heating and annealing: Synchrotron small-angle X-ray scattering study, Eur. Polym. J., 46(9) (2010) 1866-1877.

[9] E. Kretzschmar, M.D. Wolkowicz, J.-F. Enderle, D. Lilge, Preparation of transparent high density polyethylene sheets, US8029888, 2011.

[10] NOWOFOL®, NOWOFILM HD HDPE Films. https://www.nowofol.com/products/polyolefin-films/nowofilm-hd. (Accessed 1 Feb 2019).

[11] I.M. Ward, P.D. Coates, M.M. Dumoulin, Solid phase processing of polymers, Hanser Publishers, Munich, Germany, 2000.

[12] G. Capaccio, I.M. Ward, Preparation of ultra-high modulus linear polyethylenes; effect of molecular weight and molecular weight distribution on drawing behaviour and mechanical properties, Polymer, 15(4) (1974) 233-238.

[13] G. Capaccio, A. Gibson, I.M. Ward, Ultra-high modulus polymers, Applied Science Publishers, London, 1979.

[14] W. Wu, W.B. Black, High-strength polyethylene, Polym. Eng. Sci., 19(16) (1979) 1163-1169.

[15] L.E. Govaert, T. Peijs, Tensile strength and work of fracture of oriented polyethylene fibre, Polymer, 36(23) (1995) 4425-4431.

[16] P. Smith, P.J. Lemstra, Ultra-drawing of high molecular weight polyethylene cast from solution, Colloid. Polym. Sci., 258(7) (1980) 891-894.

[17] P.J. Lemstra, N.A.J.M. van Aerle, C.W.M. Bastiaansen, Chain-extended polyethylene, Polym. J., 19 (1987) 85.

[18] S. Rastogi, Y. Yao, S. Ronca, J. Bos, J. van der Eem, Unprecedented high-modulus high-strength tapes and films of ultrahigh molecular weight polyethylene via solvent-free route, Macromolecules, 44(14) (2011) 5558-5568.

[19] L. Shen, J. Severn, C.W.M. Bastiaansen, Drawing behavior and mechanical properties of ultra-high molecular weight polyethylene blends with a linear polyethylene wax, Polymer, 153 (2018) 354-361.

[20] M.P. Vlasblom, J.L.J. Van Dingenen, The manufacture, properties and applications of high strength, high modulus polyethylene fibers, Handbook of Tensile Properties of Textile and Technical Fibres, Woodhead Publishing, 2009, pp. 437-485.

[21] H. Van der Werff, U. Heisserer, High-performance ballistic fibers: ultra-high molecular weight polyethylene (UHMWPE), Advanced Fibrous Composite Materials for Ballistic Protection, Woodhead Publishing, 2016, pp. 71-107.

[22] J. Yao, C. Bastiaansen, T. Peijs, High strength and high modulus electrospun nanofibers, Fibers, 2(2) (2014) 158.

[23] T. Peijs, 1.5 High performance polyethylene fibers, in: P.W.R. Beaumont, C.H. Zweben (Eds.), Comprehensive Composite Materials II, Elsevier, Oxford, 2018, pp. 86-126.

[24] R.S. Stein, R. Prud'Homme, Origin of polyethylene transparency, J. Polym. Sci., Part B: Polym. Lett., 9(8) (1971) 595-598.

[25] L. Jarecki, D.J. Meier, Ultrahigh modulus polyethylene. II. Effect of drawing temperature on void formation and modulus, J. Polym. Sci., Part B: Polym. Phys., 17(9) (1979) 1611-1621.

[26] L. Shen, K. Nickmans, J. Severn, C.W.M. Bastiaansen, Improving the transparency of ultra-drawn melt-crystallized polyethylenes: toward high-modulus/high-strength window application, ACS Appl. Mater. Interfaces, 8(27) (2016) 17549-17554.

[27] L. Shen, J.R. Severn, C.W.M. Bastiaansen, Transparant drawn article, WO2017103055, 2017.

[28] G. Capaccio, T.A. Crompton, I.M. Ward, Drawing behavior of linear polyethylene. II. Effect of draw temperature and molecular weight on draw ratio and modulus, J. Polym. Sci., Part B: Polym. Phys., 18(2) (1980) 301-309.

[29] G. Capaccio, I.M. Ward, Effect of molecular weight on the morphology and drawing behaviour of melt crystallized linear polyethylene, Polymer, 16(4) (1975) 239-243.

[30] P. Smith, J. Lemstra Piet, P.L. Pijpers Jacques, Tensile strength of highly oriented polyethylene. II. Effect of molecular weight distribution, J. Polym. Sci., Part B: Polym. Phys., 20(12) (1982) 2229-2241.

[31] Y. Kong, J.N. Hay, The measurement of the crystallinity of polymers by DSC, Polymer, 43(14) (2002) 3873-3878.

[32] L. Jarecki, D.J. Meier, Ultra-high modulus polyethylene. 1 Effect of drawing temperature, Polymer, 20(9) (1979) 1078-1082.

[33] J.D. Ferry, Viscoelastic properties of polymers, John Wiley & Sons, 1980.

[34] C.A. Faick, A.N. Finn, The index of refraction of some soda-lime-silica glasses as a function of the composition, J. Am. Ceram. Soc., 14(7) (1931) 518-528.

[35] H. Gao, J. Li, F. Xie, Y. Liu, J. Leng, A novel low colored and transparent shape memory copolyimide and its durability in space thermal cycling environments, Polymer, 156 (2018) 121-127.

[36] N. Kurokawa, A. Hotta, Thermomechanical properties of highly transparent self-reinforced polylactide composites with electrospun stereocomplex polylactide nanofibers, Polymer, 153 (2018) 214-222.

[37] M.N. Merzlyak, K. Razi Naqvi, On recording the true absorption spectrum and the scattering spectrum of a turbid sample: application to cell suspensions of the cyanobacterium anabaena variabilis, J. Photochem. Photobiol. B: Biol., 58(2) (2000) 123-129.

[38] M. Nogi, H. Yano, Optically transparent nanofiber sheets by deposition of transparent materials: a concept for a roll-to-roll processing, Appl. Phys. Lett., 94(23) (2009) 233117.

[39] A. Peterlin, Molecular model of drawing polyethylene and polypropylene, J. Mater. Sci., 6(6) (1971) 490-508.

[40] G. Meinel, N. Morosoff, A. Peterlin, Plastic deformation of polyethylene. I. Change of morphology during drawing of polyethylene of high density, J. Polym. Sci., Part B: Polym. Phys., 8(10) (1970) 1723-1740.

[41] Y. Liu, T.P. Russell, M.G. Samant, J. Stöhr, H.R. Brown, A. Cossy-Favre, J. Diaz, Surface relaxations in polymers, Macromolecules, 30(25) (1997) 7768-7771.

[42] T. Kerle, Z. Lin, H.-C. Kim, T.P. Russell, Mobility of polymers at the air/polymer interface, Macromolecules, 34(10) (2001) 3484-3492.

[43] T. Schimanski, J. Loos, T. Peijs, B. Alcock, P.J. Lemstra, On the overdrawing of melt-spun isotactic polypropylene tapes, J. Appl. Polym. Sci., 103(5) (2007) 2920-2931.

[44] F. Mai, W. Tu, E. Bilotti, T. Peijs, The influence of solid-state drawing on mechanical properties and hydrolytic degradation of melt-spun poly(lactic acid) (PLA) tapes, Fibers, 3(4) (2015) 523.

[45] A. Peterlin, R. Corneliussen, Small-angle x-ray diffraction studies of plastically deformed polyethylene. II. Influence of draw temperature, draw ratio, annealing temperature, and time, J. Polym. Sci., Part B: Polym. Phys., 6(7) (1968) 1273-1282.

[46] M. Sumita, K. Miyasaka, K. Ishikawa, Effect of drawing on the melting point and heat of fusion of polyethylene, J. Polym. Sci., Part B: Polym. Phys., 15(5) (1977) 837-846.

[47] T. Peijs, H.A. Rijsdijk, J.M.M. de Kok, P.J. Lemstra, The role of interface and fibre anisotropy in controlling the performance of polyethylene-fibre-reinforced composites, Compos. Sci. Technol., 52(3) (1994) 449-466.

[48] T. Peijs, Composites for recyclability, Mater. Today, 4(6) (2003) 30-35.

[49] N. Cabrera, B. Alcock, J. Loos, T. Peijs, Processing of all-polypropylene composites for ultimate recyclability, Proceedings of the Institution of Mechanical Engineers, Part L: Journal of Materials: Design and Applications, 218(2) (2004) 145-155.

[50] J.M. Zhang, C.T. Reynolds, T. Peijs, All-poly(ethylene terephthalate) composites by film stacking of oriented tapes, Compos. Part A - Appl. S., 40(11) (2009) 1747-1755.

[51] B. Alcock, T. Peijs, Technology and Development of Self-Reinforced Polymer Composites, in: A. Abe, H.-H. Kausch, M. Möller, H. Pasch (Eds.), Polymer Composites – Polyolefin Fractionation – Polymeric Peptidomimetics – Collagens, Springer Berlin Heidelberg, Berlin, Heidelberg, 2013, pp. 1-76.

[52] L. Shen, J. Severn, C.W.M. Bastiaansen, Improving visible-light transparency of drawn melt-crystallized linear polyethylenes: influence of molecular weight distribution, Macromol. Mater. Eng., 302(6) (2017) 1700003.

[53] Y. Lin, W. Tu, R.C.P. Verpaalen, H. Zhang, C.W.M. Bastiaansen, T. Peijs, Transparent, lightweight and high strength polyethylene films by a scalable continuous extrusion and drawing process, Submitted (2019).

Highlights:

- Highly transparent polyethylene films are produced by adjusting drawing temperature

- The effect of drawing conditions on optical properties is systematically studied for the first time

- The films show a comparable transparency as traditional inorganic and organic glass

- The films possess high specific mechanical properties as glass fiber